Astron. Astrophys. 335, 363–369 (1998)

ASTRONOMY AND ASTROPHYSICS

Effect of varying strength and orientation of local interstellar magnetic field on configuration of exterior heliosphere: 3D MHD simulations

R. Ratkiewicz[1], **A. Barnes**[2], **G.A. Molvik**[3], **J.R. Spreiter**[4], **S.S. Stahara**[5], **M. Vinokur**[6], **and S. Venkateswaran**[6]

[1] Space Research Center, Bartycka 18A, PL-00-716 Warsaw, Poland
[2] NASA/Ames Research Center, Mail Code 245-3, Moffett Field, CA 94035-1000, USA
[3] NAI, 530 Vista Rio Court, Woodbridge, CA 95258, USA
[4] Stanford University, Stanford, CA 94305, USA
[5] RMA Aerospace, Inc., Mountain View, CA 94043, USA
[6] NASA/Ames Research Center, MS T27B-1, Moffett Field, CA 94035-1000, USA

Received 15 December 1997 / Accepted 18 February 1998

Abstract. The aim of this paper is to present the effects of varying magnitude and orientation of the local interstellar magnetic field on the heliospheric boundary region (the region between the termination shock and the bow shock containing the heliopause). Other effects such as interstellar neutrals, cosmic rays and the asymmetry of the solar wind caused by its heliolatitude dependence are disregarded. We calculate the shape and structure of the heliospheric boundary region for different interstellar Alfvénic Mach numbers and various inclination angles between Very Local InterStellar Medium (VLISM) velocity and magnetic field vectors using a fully three-dimensional MHD computational analysis. The new results show the asymmetry of this region for inclination angles $0^\circ < \alpha < 90^\circ$ and are in agreement with the Newtonian approximation theory (Fahr et al. 1986, 1988) concerning trends in the heliopause orientation and location. Unlike the NA model which only qualitatively indicates the effects of the VLISM magnetic field on the heliospheric boundary region the present 3D MHD calculations reveal fully the nature of these effects by capturing all discontinuities including the termination shock, heliopause and bow shock.

The numerical scheme employed in this study is fully implicit and conservative, using a Roe-type Riemann solver in a generalized coordinate system.

Key words: solar wind – ISM: magnetic fields – magnetic fields – MHD – plasmas – shock waves

1. Introduction

Many factors can influence the interaction between the solar wind and interstellar medium; these include magnetic fields, interstellar neutrals and ions, and galactic cosmic rays. At present their relative importance is uncertain. A fundamental aspect of the interaction of the solar wind (SW) with the very local interstellar medium (VLISM) is the dynamic equilibrium between two counterflowing plasmas (e.g. Parker 1963; Axford 1972; Baranov et al. 1979; Fahr et al. 1986, 1988; Holzer 1989; Baranov 1990; Suess 1990; Suess & Nerney 1990; Fujimoto & Matsuda 1991; Suess & Nerney 1991; Ratkiewicz 1992; Nerney et al. 1993; Washimi 1993; Steinolfson et al. 1994; Karmesin et al. 1995; Pauls et al. 1995; Brackbill & Liewer 1996; Pauls & Zank 1996; Washimi & Tanaka 1996; Zank et al. 1996; Linde et al. 1997; Pauls & Zank 1997; Pogorelov & Semenov 1997). In MHD models, the heliospheric boundary is formed by the interaction between magnetized solar wind and interstellar plasmas. This requires simulation of the three-dimensional evolution of the flow and magnetic fields. The heliospheric magnetic field has been investigated by Suess & Nerney (1990, 1991), Nerney et al. (1993), Suess & Smith (1996), Suess et al. (1996). Studies of solar magnetic field effects and/or galactic neutral particles including the interstellar magnetic field perpendicular or parallel to the VLISM velocity have been conducted by Washimi (1993), Brackbill & Liewer (1996), Washimi & Tanaka (1996), Linde et al. (1997), Pogorelov & Semenov (1997).

The solar wind parameters are relatively well known, but our knowledge of the interstellar medium is presently incomplete. A large uncertainty concerns the magnetic field whose magnitude as well as direction are only crudely determined (e.g., Gloeckler et al. 1997). Therefore, in MHD modeling of the heliosphere, the interstellar magnetic field intensity and its direction may be regarded as free parameters. The computational analysis should then encompass the entire range of inclination angle α defined as the angle between the interstellar velocity $\mathbf{V_{is}}$ and the magnetic field $\mathbf{B_{is}}$ vectors, and various Alfvénic Mach numbers, relating to the magnetic field strength.

The only study of the effects of varying strength and orientation of the interstellar magnetic field on the configuration of the exterior heliosphere has been carried out by Fahr et al. (1986,1988) using the so called Newtonian approximation

Send offprint requests to: R. Ratkiewicz

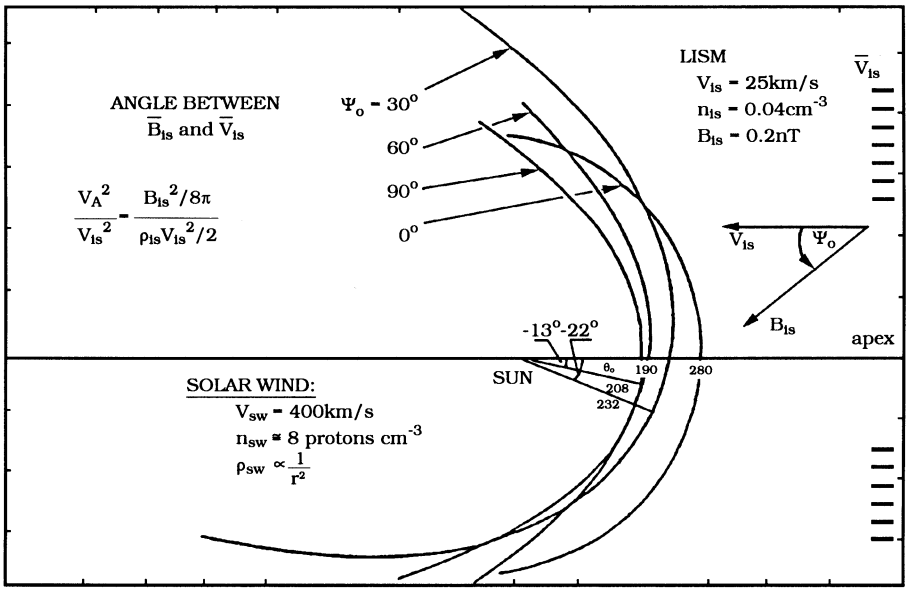

Fig. 1. Shape of frontal NA 'heliopause' in the fundamental plane of symmetry for angle between VLISM velocity ($-\mathbf{V_{is}}$) and magnetic field ($\mathbf{B_{is}}$) ψ_0 equal to 0°, 30°, 60°, and 90° (from Fahr et al. 1986). Note that in this figure $\psi_0 = -\alpha$.

(NA). In the NA approach a single surface is defined, called the 'heliopause' that represents the termination shock, the real heliopause and the bow shock. The basic assumption of the NA is that normal components of the total unperturbed hydromagnetic momentum flux on the both sides of this 'heliopause' are equal. It has been shown that, in the fundamental plane of symmetry defined by the VLISM velocity and magnetic field vectors, the nose of the 'heliopause' changes position when the inclination angle is varied (Fig. 1). The axis connecting the nose of the 'heliopause' and the Sun deviates from the apex direction (from which the interstellar plasma is moving) by an angle θ_0, which is a simple function of the intensity of the magnetic field (or Alfvénic Mach number $M_A = V/V_A, V_A = B/\sqrt{4\pi\rho}$) and the inclination angle α:

$$\theta_0 = (1/2)\tan^{-1}[(1/M_A^2)\sin 2\alpha/(1-(1/M_A^2)\cos 2\alpha)]$$

(note that in Fig. 1 the inclination angle called ψ_0 is defined as an angle between $-\mathbf{V_{is}}$ and $\mathbf{B_{is}}$, hence $\psi_0 = -\alpha$). In addition, the distance from the Sun to the nose of the 'heliopause' also depends on the inclination angle and, for each fixed M_A, attains a minimum value for 90° and maximum for 0° inclination.

The current paper presents the three-dimensional MHD computational analysis of the effects of varying strength and orientation of the local interstellar magnetic field on the heliospheric configuration. The effects of interstellar neutrals, cosmic rays and the heliolatitude dependence of the solar wind are disregarded. The 3D MHD calculations reveal the full structure of the flow and the magnetic fields, and capture all discontinuities including the termination shock, heliopause and bow shock. The algorithm has been validated for the heliospheric interaction in the gasdynamic limit (i.e. zero magnetic field), using the results of Baranov et al. (1979). While detailed validation of the MHD results is currently limited because of differences in the assumptions of available models (Brackbill & Liewer 1996; Linde et al. 1997), the predicted results are observed to be in qualitative agreement with the trends of the NA model.

The MHD results reported in this paper show fully the nature of the asymmetry of the heliospheric boundary region which arises for inclination angles $0^\circ < \alpha < 90^\circ$. They also reveal new aspects of the VLISM magnetic field influence on the shape and structure of the heliospheric boundary as discussed in Sect. 4.

2. Governing MHD equations

We consider ideal MHD interaction between solar wind and VLISM plasmas. In this case the fundamental assumption underlying this interaction is that the average dependent variables of the flowing plasma can be adequately described by the continuum equations of magnetohydrodynamics for a single component perfect gas having infinite electrical conductivity and zero viscosity and thermal conductivity. The magnetohydrodynamic equations express the conservation of mass, momentum, energy and magnetic field. These equations may be written in a conservative variable form as (e.g. Jeffrey and Taniuti 1964; Powell et al. 1995):

$$\frac{\partial \mathbf{U}}{\partial t} + \nabla \cdot \bar{\mathbf{F}} = \mathbf{0} \tag{1}$$

where $\mathbf{U}$, a column vector, and $\bar{\mathbf{F}}$, a flux tensor are defined as:

$$\mathbf{U} = \begin{vmatrix} \rho \\ \rho\mathbf{u} \\ \mathbf{B} \\ \rho E \end{vmatrix} \qquad \bar{\mathbf{F}} = \begin{vmatrix} \rho\mathbf{u} \\ \rho\mathbf{u}\mathbf{u} + \mathbf{I}(p + \frac{\mathbf{B}\cdot\mathbf{B}}{8\pi}) - \frac{\mathbf{B}\mathbf{B}}{4\pi} \\ \mathbf{u}\mathbf{B} - \mathbf{B}\mathbf{u} \\ \rho H\mathbf{u} - \frac{\mathbf{B}(\mathbf{u}\cdot\mathbf{B})}{4\pi}) \end{vmatrix}$$

where ρ is the density, p is the pressure, $\mathbf{u}$ is the velocity vector, $\mathbf{B}$ is the magnetic field vector, $E = \frac{1}{\gamma-1}\frac{p}{\rho} + \frac{\mathbf{u}\cdot\mathbf{u}}{2} + \frac{\mathbf{B}\cdot\mathbf{B}}{8\pi\rho}$ is the total energy, $H = \frac{\gamma}{\gamma-1}\frac{p}{\rho} + \frac{\mathbf{u}\cdot\mathbf{u}}{2} + \frac{\mathbf{B}\cdot\mathbf{B}}{4\pi\rho}$ is the total enthalpy, γ is the ratio of specific heats and $\mathbf{I}$ is the 3 x 3 identity matrix.

The additional constraint of a divergence-free magnetic field, $\nabla \cdot \mathbf{B} = 0$, must also be satisfied. It follows rigorously from the Maxwell equations that a divergence-free magnetic field will be maintained for all time if the initial field is divergence-free. However, it is not straightforward to implement this condition numerically, since various numerical errors tend to destroy the divergence-free magnetic field condition. Recently, Powell et al. (1995) have suggested a procedure in the development of upwind schemes for the MHD equations to ensure that the magnetic field remains divergence-free. This is accomplished by adding a source term $\mathbf{Q}$ to the RHS of (1), which is proportional to the divergence of the magnetic field (Brackbill & Barnes 1980; Powell et al. 1995; Ratkiewicz, in prep.):

$$\frac{\partial \mathbf{U}}{\partial t} + \nabla \cdot \bar{\mathbf{F}} = \mathbf{Q} \qquad \mathbf{Q} = - \begin{vmatrix} 0 \\ \frac{\mathbf{B}}{4\pi} \\ \mathbf{u} \\ \mathbf{u} \cdot \frac{\mathbf{B}}{4\pi} \end{vmatrix} \nabla \cdot \mathbf{B} \qquad (2)$$

From an analytical viewpoint only terms equal to zero are added to the original set of governing equations. Numerically, however, when $\nabla \cdot \mathbf{B} \neq 0$ occurs locally during the solution procedure, the artificial source terms in (2) provide an effective method of convecting these errors out of the system and restoring the divergence-free condition.

3. Numerical algorithm and boundary conditions

The fully conservative three-dimensional set of equations describing the interaction of the solar wind with the interstellar magnetized plasma is solved using a spatial first order time-marching, implicit, upwind-differenced scheme based on a finite-volume approach (Hirsch, 1988). Computations begin from an assumed initial state corresponding to a specified VLISM flow everywhere and proceed to convergence for a specified set of solar wind properties and for a sequence of inclination angles. The runs presented here have each taken 25-40 hours (on a workstation Alpha DEC 3000) to reach a steady-state. The grid that is used for the computations is generated internally in the 3D MHD code, and is a spherical one containing 40 grid points in the azimuthal i-direction (θ), 80 points in the radial j-direction (r), and 20 points in the meridional k-direction (ψ). As a test we also calculated a model for a 80 x 160 x 20 grid and the results were indistinguishable. Additional details of the algorithm are described by Molvik et al. (1996). The present numerical study adopts a cell-centered finite volume representation of the conservation equations. This means that the solution variables are stored at the cell centers. For the spherical coordinate system used here, this means that the variables are not stored along the centerline (which forms a cell face). Also, since the centerline represents a cell-face of zero area to the adjacent cell-volumes, the boundary condition requires that the fluxes are zero through this cell face. Thus, the field variables along the centerline are not required in the flux computations and, consequently, they are not calculated or stored. Therefore, in displaying the results, the centerline section is not plotted. We point out that this boundary

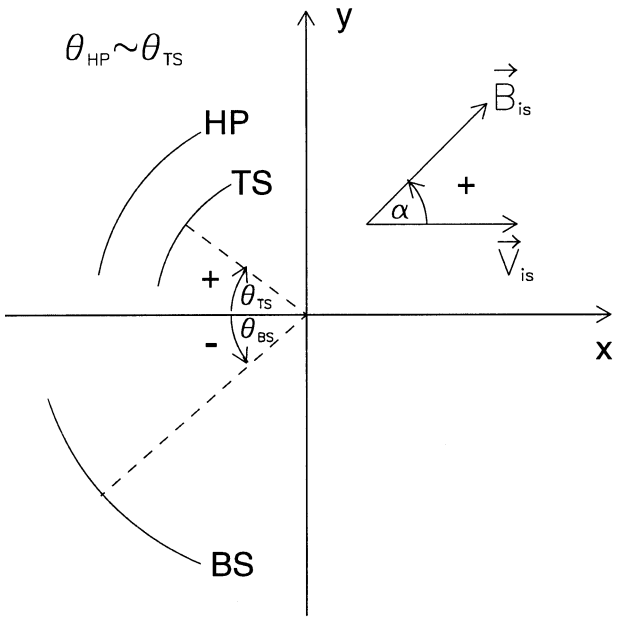

Fig. 2. Schematic representation of the VLISM velocity ($\mathbf{V_{is}}$) and magnetic field ($\mathbf{B_{is}}$) configuration. The position of the termination shock, heliopause and bow shock noses are also schematically shown.

treatment is standard in cell-centered finite volume schemes and should not cause any non-physical behaviour.

The inner and outer boundaries are spheres placed at $r_0 = 30AU$ and at $R_{out} \sim 15000AU$, respectively. The boundary conditions for the solar wind at the inner boundary are: number density $n_0 = 0.011cm^{-3}$, velocity $V_0 = 400kms^{-1}$, Mach number $M_0 = 10$. We have assumed the interplanetary magnetic field is small (i.e. $B^2/8\pi \ll \rho v^2$ in the unshocked solar wind and $B^2/8\pi \ll p$ in the shocked solar wind) and have disregarded it. This assumption enables us to make a thorough study of the influence of the interstellar magnetic field on the shape of the heliospheric boundary region. For the interstellar magnetized plasma, at the outer boundary the boundary conditions are: fixed number density $n_{is} = 0.1cm^{-3}$, velocity $V_{is} = 26kms^{-1}$ and Mach number $M_{is} = V_{is}/C_{is} = 1.6$, where C_{is} is the interstellar sound speed, and Alfvénic Mach number M_A varying from 1.5 to 15, and inclination angle $\alpha = 0°, 30°, 60°, 90°$. The Cartesian coordinate system, which is centered on the Sun and defined as: $x = -r\cos\theta$, $y = r\sin\theta\cos\psi$, $z = r\sin\theta\sin\psi$ is chosen in such a way that the XY plane contains the VLISM velocity vector $\mathbf{V_{is}}$ and VLISM magnetic field vector $\mathbf{B_{is}}$ (Fig. 2). Hence, $B_{xo} = B_{is}\cos\alpha$, $B_{yo} = B_{is}\sin\alpha$ and $B_{zo} = 0$. The flows are taken to be adiabatic with $\gamma = 5/3$ throughout.

4. Results and discussion

For all cases of the inclination angle, including zero degrees (axi-symmetric case), the results for the pressure, density, velocity and the magnetic field are obtained with the new 3D MHD solver. In order to show the nature of asymmetry of the heliospheric boundary region caused by the interstellar magnetic field, we display all results in the XY plane, using contour plots.

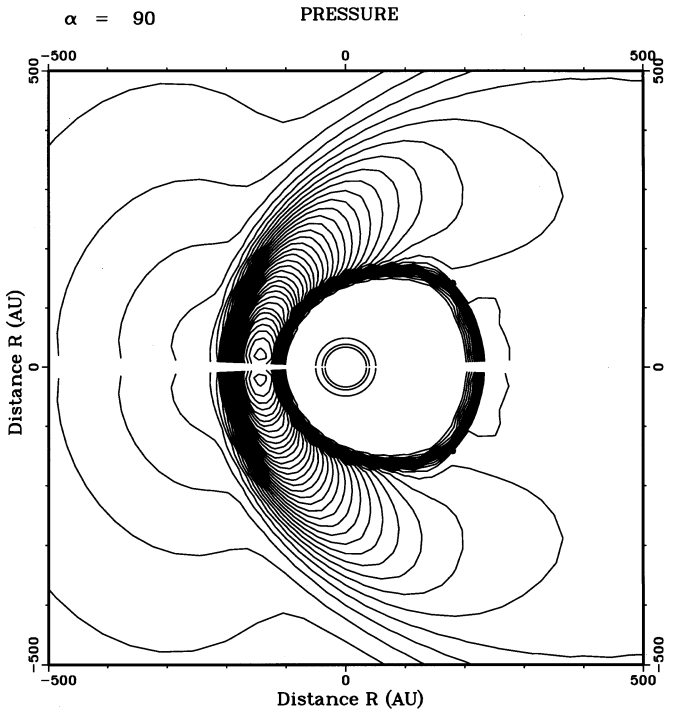

Fig. 3. Shape and size of the heliosphere as shown by thermal pressure contour plots in the XY plane (containing VLISM velocity vector $\mathbf{V_{is}}$ and VLISM magnetic field vector $\mathbf{B_{is}}$) for 90° shock limit ($M_A = 1.5$).

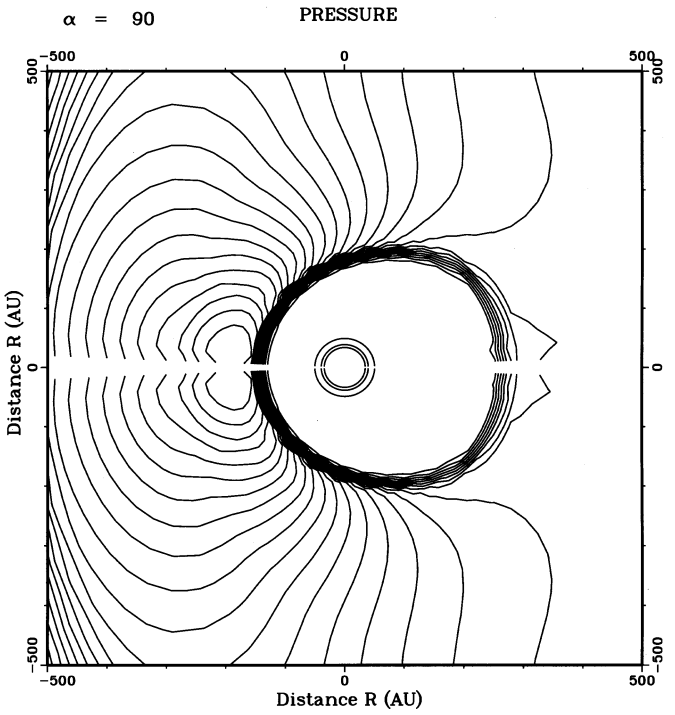

Fig. 4. As Fig. 3 but gasdynamic limit.

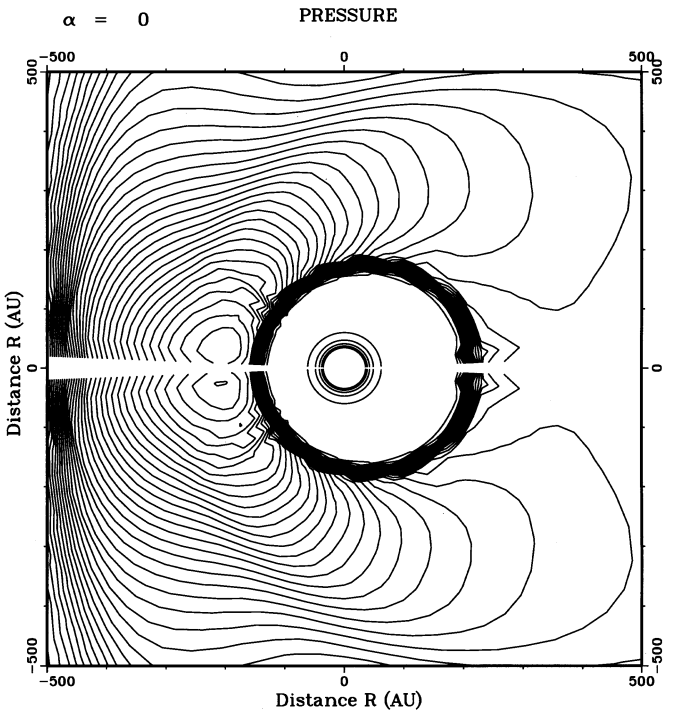

Fig. 5. As Fig. 3 but 0° shock limit ($M_A = 1.5$).

In all computations the interstellar Mach number is fixed at 1.6 (supersonic flow), while we vary the VLISM inclination angle and Alfvénic Mach number. All dependent variables (except pressure) are normalized in terms of their values at the outer boundary. Pressure is expressed in terms of the dynamic pressure ρV^2 at the outer boundary. The 3D MHD calculations show the shape and the structure of the heliospheric boundary region including the termination shock, the heliopause and the bow shock.

Table 1 summarizes the results for two different interstellar Alfvénic Mach numbers: 1.5 (MHD case) and 15 (which approaches the gasdynamic limit). The approximate heliocentric distances to the termination shock (TS), heliopause (HP), and bow shock (BS) noses are displayed. To be explicit, we define the noses for a superAlfvénic interstellar plasma as follows: noses of the termination shock, the heliopause and the bow shock are the closest points to the Sun in the upwind direction relative to the interstellar wind. The nose of the heliopause is also the point at which the total pressure attains a maximum.

In the three last rows of Table 1 we show the deviation angles from the apex direction: θ_{TS} for the termination shock, θ_{HP} for the heliopause, and θ_{BS} for the bow shock noses. The distances shown in the right most column are in very good agreement with those obtained by Baranov et al. (1979) using a gasdynamic model. The results displayed in the columns 5 and 6 (both for 90°) together with inspection of Figs. 3 and 4 show that the heliosphere is compressed under the influence of the magnetic field resulting in the additional magnetic pressure acting on the heliosphere. The heliocentric distance of the heliopause and the termination shock noses strongly depends on the inclination angle and is smaller for 90° than for 0° (Figs. 3 and 5), as consistent with NA. However, the full MHD simulation shows that the bow shock displays the tendency to move out farther from the Sun and becomes weaker for larger inclination angles.

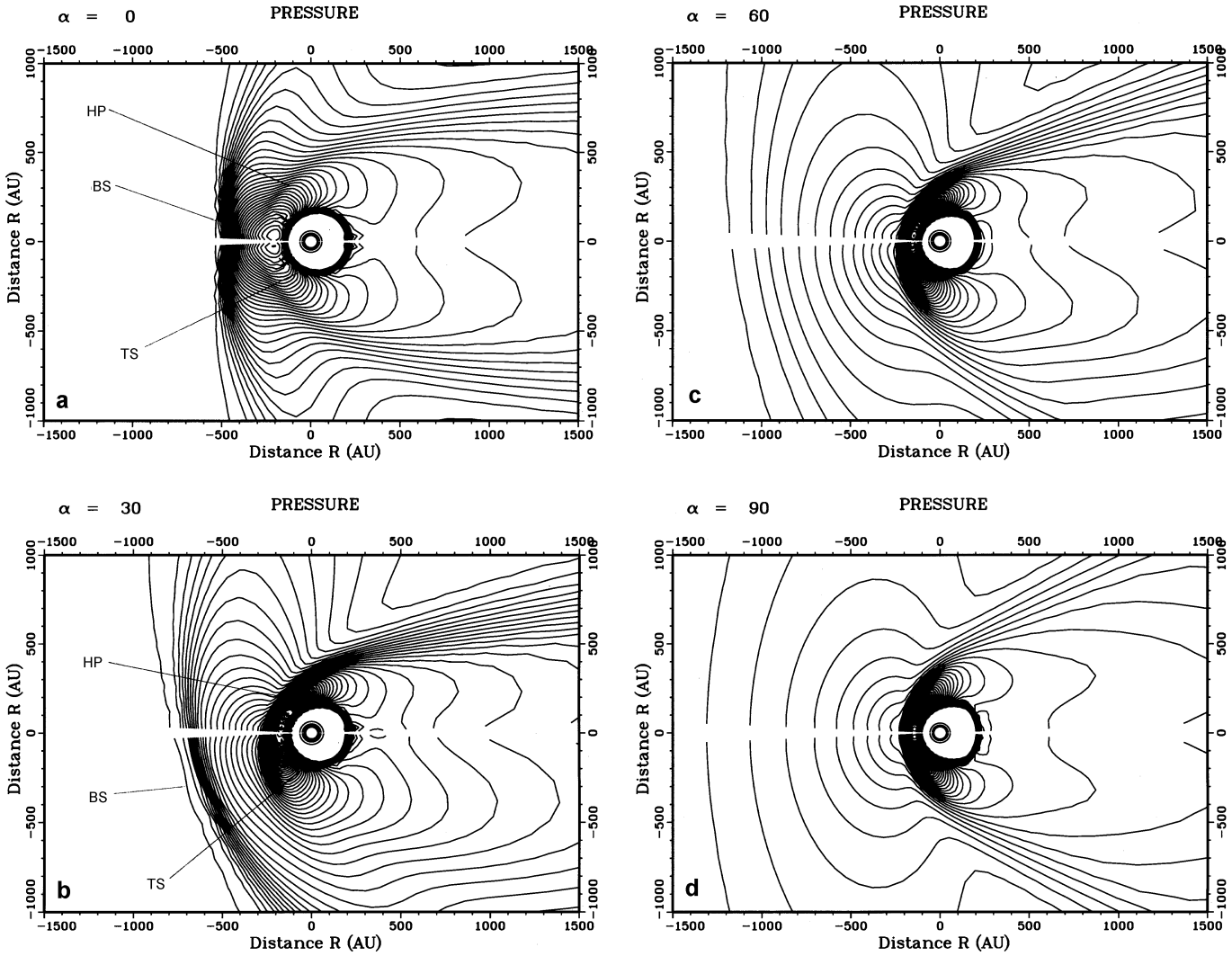

Fig. 6a–d. Shape of the heliospheric boundary region as shown by thermal pressure contour plots for inclination angle α equal to **a** 0°, **b** 30°, **c** 60°, **d** 90°. VLISM Alfvénic Mach number = 1.5. Positions of termination shock (TS), heliopause (HP) and bow shock (BS) are as indicated in Figs. 6a and 6b.

Table 1. Distances and deviation angles of TS, HP and BS noses

M_A	1.5				15
α	0°	30°	60°	90°	90°
$TS(AU)$	150	130	115	105	150
$HP(AU)$	290	240	220	200	250
$BS(AU)$	540	700	1200	1700	620
θ_{TS}	0°	19°	10°	0°	0°
θ_{HP}	0°	19°	10°	0°	0°
θ_{BS}	0°	-20°	-12°	0°	0°

These numbers are obtained by the visual inspection of the numerical results. The uncertainties of numbers in this table are less than 3° for the deviation angles other than 0°, and less than $10AU$ for distances. θ_{TS} and θ_{HP} are approximately the same.

This result could not of course be anticipated from a simple NA model. The changes in the configuration of the heliospheric boundary region are shown in Fig. 6a-d by thermal pressure contour plots with an inclination angle α equal to 0°, 30°, 60°, 90°, and VLISM Alfvénic Mach number = 1.5. The positions of the termination shock, the heliopause and the bow shock are as indicated in Fig. 6a-b. In Figs. 6c and 6d the termination shock and the heliopause are clearly visible, but the bow shock has become very weak. Physically, because the inclination angle is close to 90°, the bow shock would be a quasi-perpendicular MHD shock near the nose. The upstream magnetosonic Mach number $M_{F\perp} = \sqrt{V_{is}^2/(C_{is}^2 + V_A^2)}$ is ~ 1.09. This number is near 1, so that the bow shock must be weak (Jeffrey & Taniuti 1964).

For an inclination angle equal to 0° (Fig. 6a), the heliospheric boundary is axisymmetric. When the inclination angle changes to 30° (Fig. 6b), there is a substantial change in its configuration. The heliopause and termination shock noses move in one direction, while the nose of the bow shock moves in the opposite direction. This is a new and interesting result for the

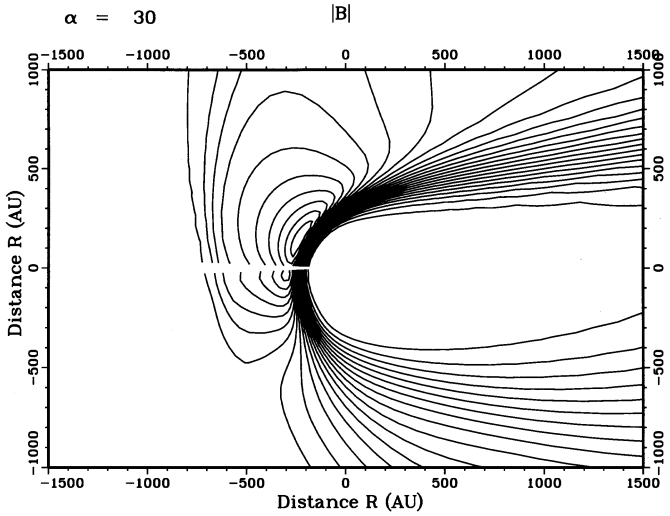

Fig. 7. Asymmetric enhancement of VLISM magnetic field as shown by magnetic field absolute value contour plots for inclination angle α equal to 30°.

heliospheric configuration, not obtainable by a simplified NA approach. Similar result has been found for a bow shock at the Earth's magnetosphere (Spreiter & Stahara 1994), confirmed by further magnetospheric calculations by Stahara and Spreiter (private communication). Fig. 7 shows that maximum compression of the shocked (oblique) VLISM field occurs at a point lying near the direction of closest approach to the Sun by the unperturbed VLISM fieldlines. The gas pressure (Fig. 6b) behaves in a similar way, so that the maximum of the total pressure, $p + B^2/8\pi$, is shifted upward. Since the total pressure must be the same at both sides of the heliopause, the compressed solar wind adjusts accordingly to it, shifting both boundaries (TS and HP). Simultanously the bow shock becomes weaker in this region, as described earlier, and moves away from the Sun. The closest point of the bow shock is pushed in the opposite direction to the closest points of the heliopause and the termination shock ('down' in our figures). This asymmetry is reduced for an angle of 60° (Fig. 6c); for 90° (Fig. 6d) the nose directions are aligned once again. The asymmetry of the heliospheric boundary depends not only on the inclination angle but also on the strength of the interstellar magnetic field measured by the Alfvénic Mach number M_A as already shown by the NA approximation. The change in shape of the termination shock is also a function of the inclination angle and the strength of the magnetic field..

5. Concluding remarks

This paper shows the 3D MHD results for an *arbitrary* interstellar magnetic field inclination angle. The solutions capture all discontinuities including the termination shock, heliopause and bow shock, and show several important features of complexity of the interaction between the solar wind and the interstellar magnetized plasma. The results reveal the nature of the influence of the interstellar magnetic field on the shape and structure of the heliospheric boundary region:

(a) The heliosphere is compressed under the influence of the interstellar magnetic field.

(b) The magnetic field tension $(\mathbf{B}\cdot\nabla)\mathbf{B}/4\pi$ and pressure $B^2/8\pi$ cause the asymmetry for inclination angles other than 0° or 90° pushing the heliopause and the termination shock noses in one direction, and the bow shock nose in the opposite direction; the asymmetry depends on the inclination angle and the strength of the VLISM magnetic field.

(c) For inclination angles close to 90° the magnetic field pressure $B^2/8\pi$ causes the distance between the bow shock and the heliopause to increase and the bow shock to weaken. As the result the heliocentric distance of the bow shock attains its minimum for an inclination angle of 0° while the maximum occurs at 90°.

(d) In contrast, minimum heliocentric distances of the heliopause and the termination shock occur when the inclination angle is 90°, and the maximum occurs at 0°.

Acknowledgements. This research was carried out during the tenure of one of the authors (R. R.) as a National Research Council Resident Research Associate at the Ames Research Center. This research was also supported in part by NASA Requisition No. SST 3988 (for G. A. M.) and by the Independent Research and Development Program at RMA Aerospace, Inc. (for S. S. S. & J. R. S.). The authors wish to thank J. D. Mihalov, W. Davies, and P. R. Gazis for reviewing earlier versions of this paper and J. F. McKenzie and M. Lee for fruitful discussions.

References

Axford, W.I., 1972, In: Solar Wind, NASA SP-308, 609, C.P. Sonett, P.J. Coleman, Jr., J.M. Wilcox, eds

Baranov, V.B., 1990, Space Sci. Rev. 52, 89

Baranov, V.B., Lebedev, M.G, Ruderman, M.S., 1979, Ap&SS 66, 441

Brackbill, J.U., Barnes, D.C., 1980, J. Comp. Physics 35, 426

Brackbill, J.U., Liewer, P.C., 1996, Poster paper SH31A-24, AGU 1996 Fall Meeting, San Francisco, Supplement to EOS Transactions, AGU, Vol. 77, No 46

Fahr, H.J., Ratkiewicz, R., Grzedzielski, S., 1986, Adv. Space Res. 6, No. 1, 389

Fahr, H.J., Grzedzielski, S., Ratkiewicz, R., 1988, Annales Geophysicae 6,(4), 337

Fujimoto, Y., Matsuda, T., 1991, KUGD91-2, Department of Aeronautical Engineering, Kyoto University, Kyoto 606, Japan

Gloeckler, G., Fisk, L. A., Geiss, J., 1997, Nat, 386, 374

Hirsch, C., 1988, Numerical computation of Internal and External Flows, Vol. I and II, John Wiley & Sons

Holzer, T.E., 1989, ARA&A 27, 199

Jeffrey, A, Taniuti, T., 1964, Non-linear wave propagation, Academic Press

Karmesin, S.R., Liewer, P.C., Brackbill, J.U., 1995, Geophys. Res. Lett. 22, 1153

Linde, T.J., Gombosi, T.I., Roe, P.L., Powell, K.G., DeZeeuw, D.L., 1997, The Heliosphere in the Magnetized Local Interstellar Medium: Results of a 3D MHD Simulation, submitted to JGR

Molvik, G.A., Stahara, S.S., Spreiter, J.R., Vinokur, M., Ratkiewicz, R., 1996, Final Report of National Aerosciences Institute, Ref. No. SST3988

Nerney, S., Suess, S.T., Schmahl, E.J., 1993, J. Geophys. Res. 98, A9, 15169
Parker, E.N., 1963, Interplanetary Dynamical Processes, Intersience Publishers
Pauls, H.L., Zank, G.P., Williams, L.L., 1995, J. Geophys. Res. 100, 21595
Pauls, H.L., Zank, G.P., 1996, J. Geophys. Res. 101, 17,081
Pauls, H.L., Zank, G.P., 1997, J. Geophys. Res., 102, 9, 19779
Pogorelov, N.V., Semenov, A.Yu., 1997, A&A 321, 330
Powell, K.G., Roe, P.L., Myong, R.S., Gombosi, T., DeZeeuw, D.L., 1995, An upwind scheme for magnetohydrodynamics, AIAA Paper 95-1704-CP
Ratkiewicz, R., 1992, A&A 255, No 1/2, 383
Spreiter, J.R., Stahara, S.S., 1994, Adv. Space Res., 14, No. 7, (7)5
Steinolfson, R.S., Pizzo, V.J., T. Holzer, T., 1994, Geophys. Res. Letters 21, No. 4, 245
Suess, S.T., 1990, Rev. Geophys. 28, 97
Suess, S.T., Nerney, S.F., 1990, J. Geophys. Res. 95, 6403
Suess, S.T., Nerney, S.F., 1991, J. Geophys. Res. 96, 1883
Suess, S.T., Smith, E.J., 1996, Geophys. Res. Letters, 23, No. 22, 3267
Suess, S.T., Smith, E.J., Phillips, J., Goldstein, B.E., Nerney, S.F., 1996, A&A (submitted)
Washimi, H., 1993, Adv. Space Res. 13(6), 227
Washimi, H., Tanaka, T., 1996, Space Sci. Reviews 78, 85
Zank, G.P., Pauls, H.L., Williams, L.L., Hall, D.T., 1996, J. Geophys. Res. 101, 21639